Supplementary Information

Tuning of the elastic modulus of a soft polythiophene through molecular doping

Sepideh Zokaei,[a†*] Donghyun Kim,[b†] Emmy Järsvall,[a†] Abigail M. Fenton,[c] Albree R. Weisen,[c] Sandra Hultmark,[a] Phong H. Nguyen,[d] Amanda M. Matheson,[e] Anja Lund,[a] Renee Kroon,[a,b,f] Michael L. Chabinyc,[e] Enrique D. Gomez,[c,g] Igor Zozoulenko[b,f] and Christian Müller[a,h*]

[a]Department of Chemistry and Chemical Engineering, Chalmers University of Technology, 41296 Göteborg, Sweden

[b]Laboratory of Organic Electronics, Linköping University, 60174 Norrköping, Sweden

[c]Department of Chemical Engineering, The Pennsylvania State University, University Park, Pennsylvania 16802, USA

[d]Department of Chemical Engineering, University of California, Santa Barbara, California 93106, USA

[e]Materials Department, University of California, Santa Barbara, 93106 California, USA

[f]Wallenberg Wood Science Center, Linköping University, 60174 Norrköping, Sweden

[g]Department of Materials Science and Engineering, The Pennsylvania State University, University Park, Pennsylvania 16802, USA

[h]Wallenberg Wood Science Center, Chalmers University of Technology, 41296 Göteborg, Sweden

[†]These authors contributed equally.

*e-mail: zokaei@chalmers.se, christian.muller@chalmers.se

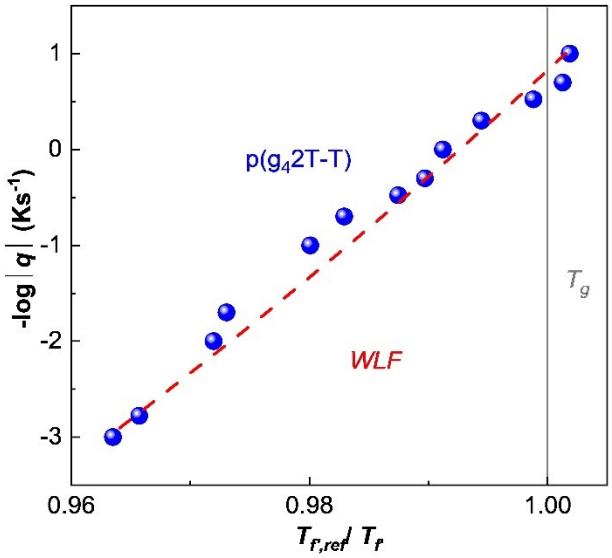

Fig. S1. Angell plot for p(g$_4$2T-T) showing $-\log q$ vs. $T_{f,ref}^{'}/T_{f}^{'}$; the fictive temperature $T_{f}^{'}$ was determined with fast scanning calorimetry (FSC) for cooling rates ranging from q = -0.1 to -1000 K s^{-1} and the reference fictive temperature $T_{f,ref}^{'} = T_g$ was measured with conventional differential scanning calorimetry (DSC) using q_{ref} = -0.17 K s^{-1}; the experimental data (blue spheres) were fited with the Williams–Landel–Ferry (WLF) equation $log(q/q_{ref}) = -C_1\left(T_f - T_{f,ref}^{'}\right)/\left[C_2 + \left(T_f - T_{f,ref}^{'}\right)\right]$ yielding $C_1 \approx 28$ and $C_2 \approx 68$ K (red dashed line.[1]

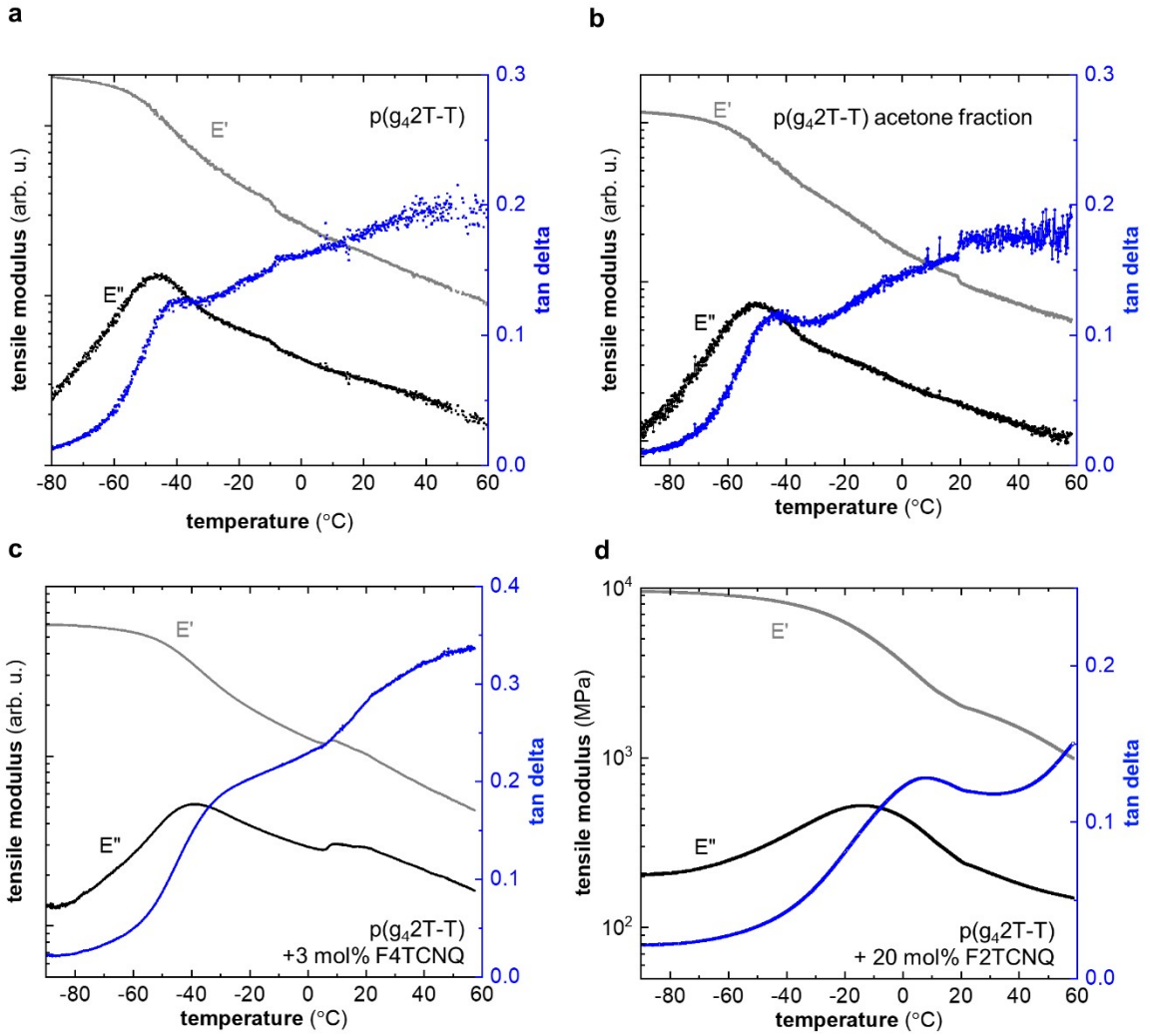

Fig. S2. Tensile storage and loss modulus, $E^{'}$ and $E^{''}$, and $\tan\delta = E^{''}/E^{'}$ measured by supporting the material by glass mesh with strands cut at 45° of (a) p($g_4$2T-T) before doping, (b) the low molecular-weight fraction of p($g_4$2T-T) collected through fractionation with acetone after synthesis, (c) p($g_4$2T-T) doped with 3 mol% F4TCNQ and supported by a glass mesh, and (d) p($g_4$2T-T) doped with 20 mol% F4TCNQ (free-standing film) as a function of temperature.

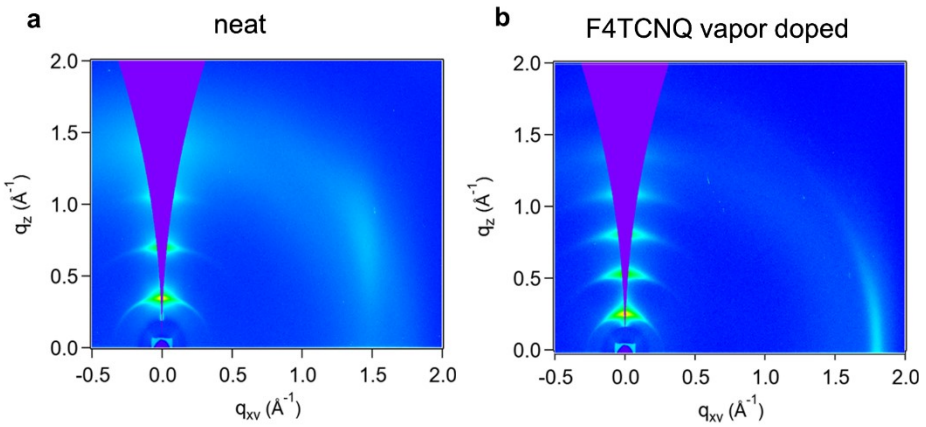

Fig. S3. GIWAXS pictograms of p($g_4$2T-T) (a) before and (b) after vapor doping with F4TCNQ.

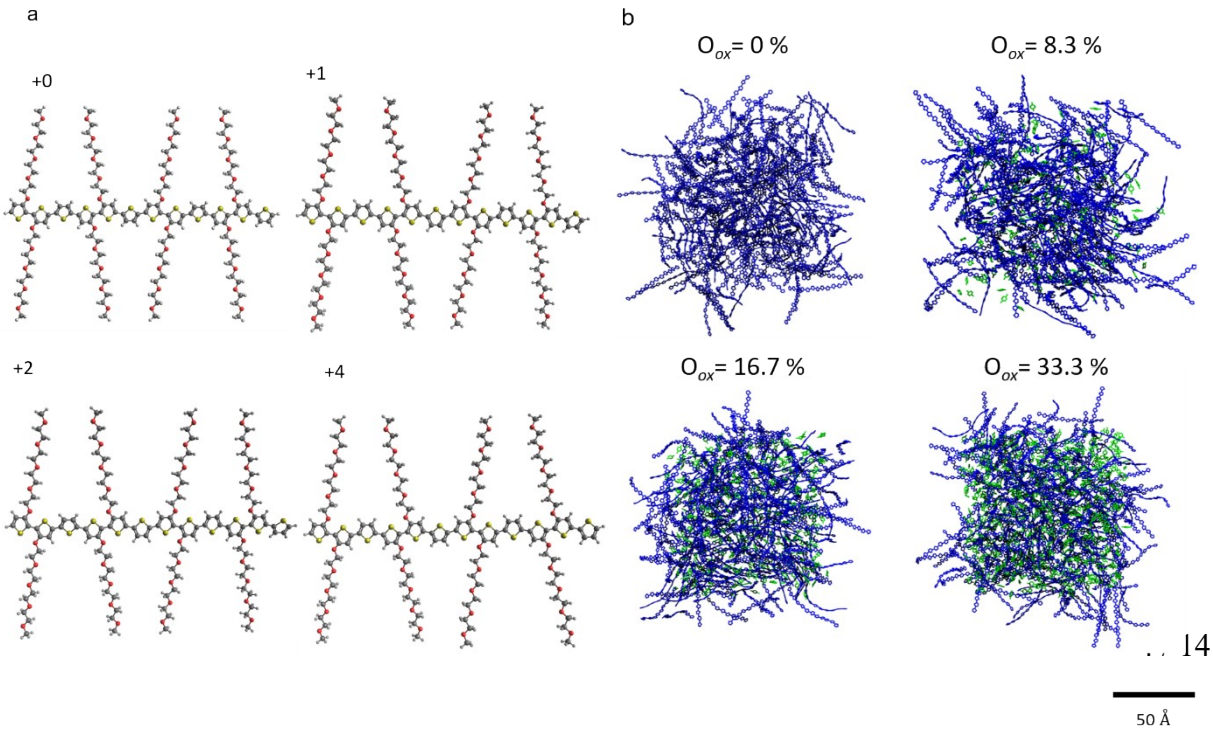

Fig. S4. (a) Initial structure of oligomers with 4 $g_4$2T-T repeat units with charge 0, +1, +2, or +4 used for MD simulations obtained by Geometry Optimization in DFT; (b) Snapshots of films obtained from MD simulations with respect to oxidation level. Note that polymers and counterions are illustrated with blue and green lines, respectively, and the side chains of polymers are omitted.

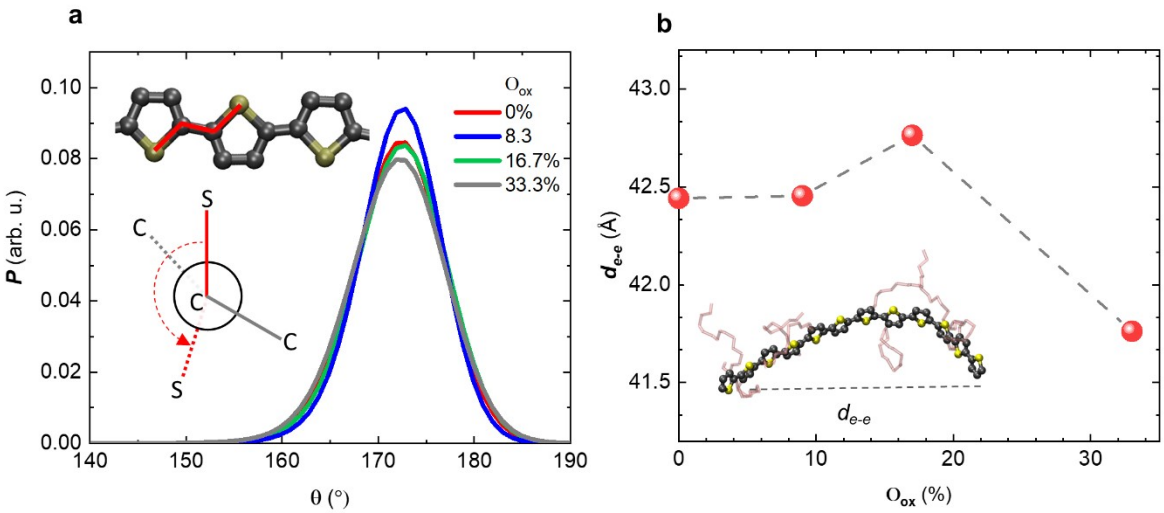

Fig. S5. (a) Dihedral angle (θ) of -*S*-*C*-*C*-*S*- within an oligomer chain; (b) average end-to-end distance ($d_{e\text{-}e}$) of oligomer chains.

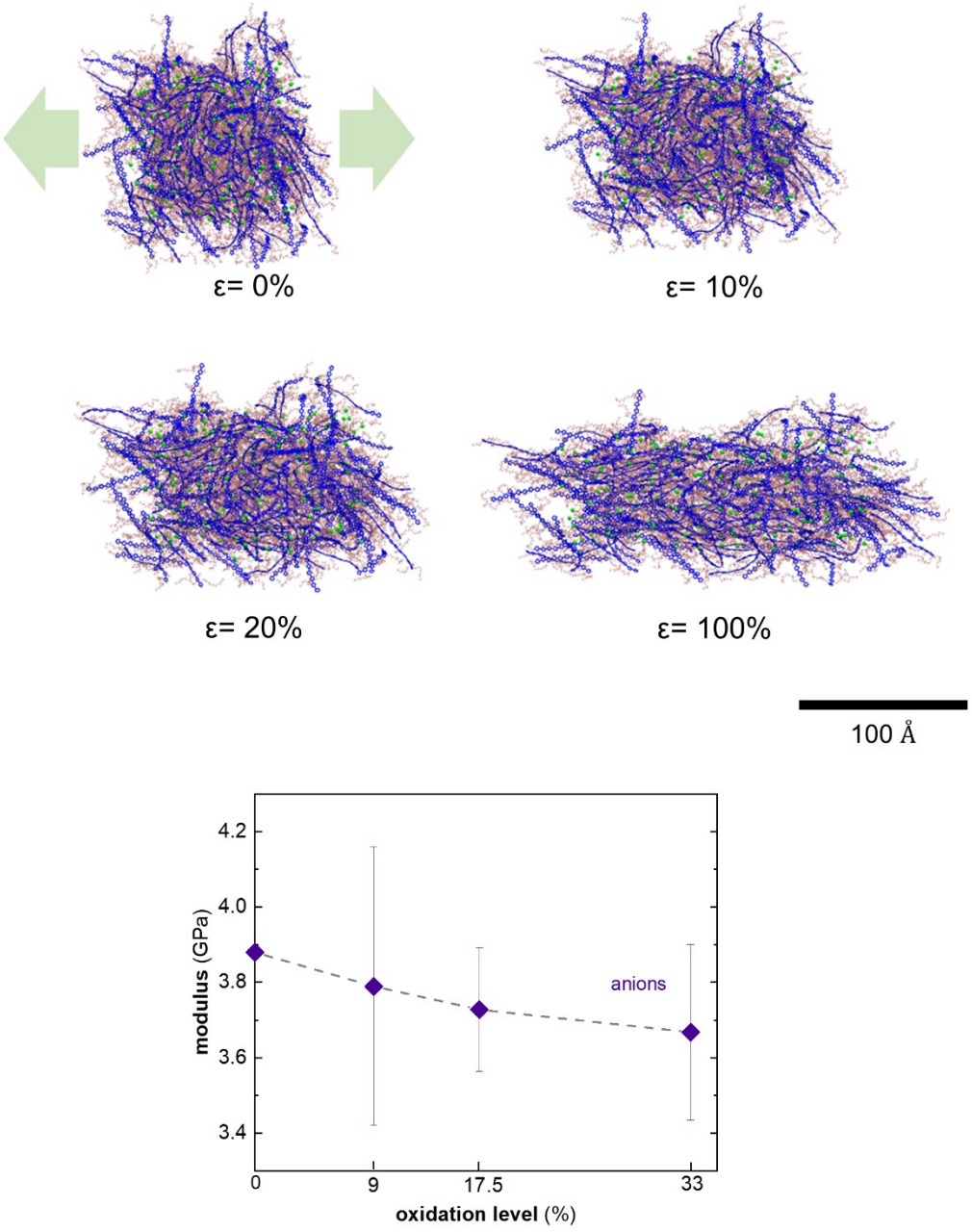

Fig. S6. Simulation of film deformation. (a) Morphology at $^{O}_{ox}$ = 8.3% with F4TCNQ anions as counterions and an applied strain ε = 0, 10, 20, 100%. The main chains and side chains are represented by blue and pink lines, respectively. Green spheres are counterions. (b) Young's modulus as function of oxidation level.

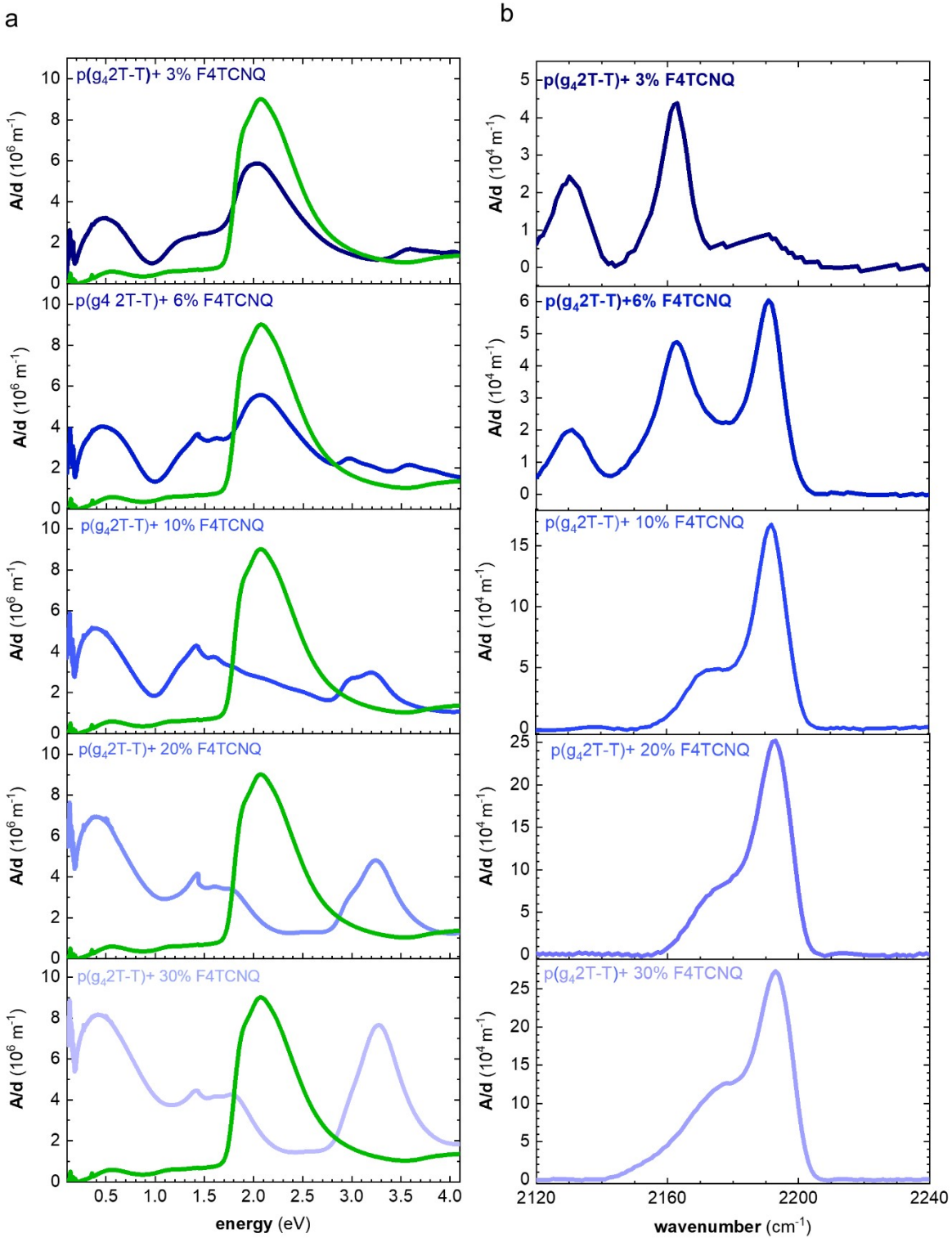

Fig. S7. a) Uv-vis and (b) Transmission FTIR absorbance spectra, with the absorbance A normalized by the film thickness d, of p($g_4$2T-T) before (green) and after doping with 3 mol%, 6 mol%, 10 mol%, 20 mol% and 30 mol% F4TCNQ (blue).

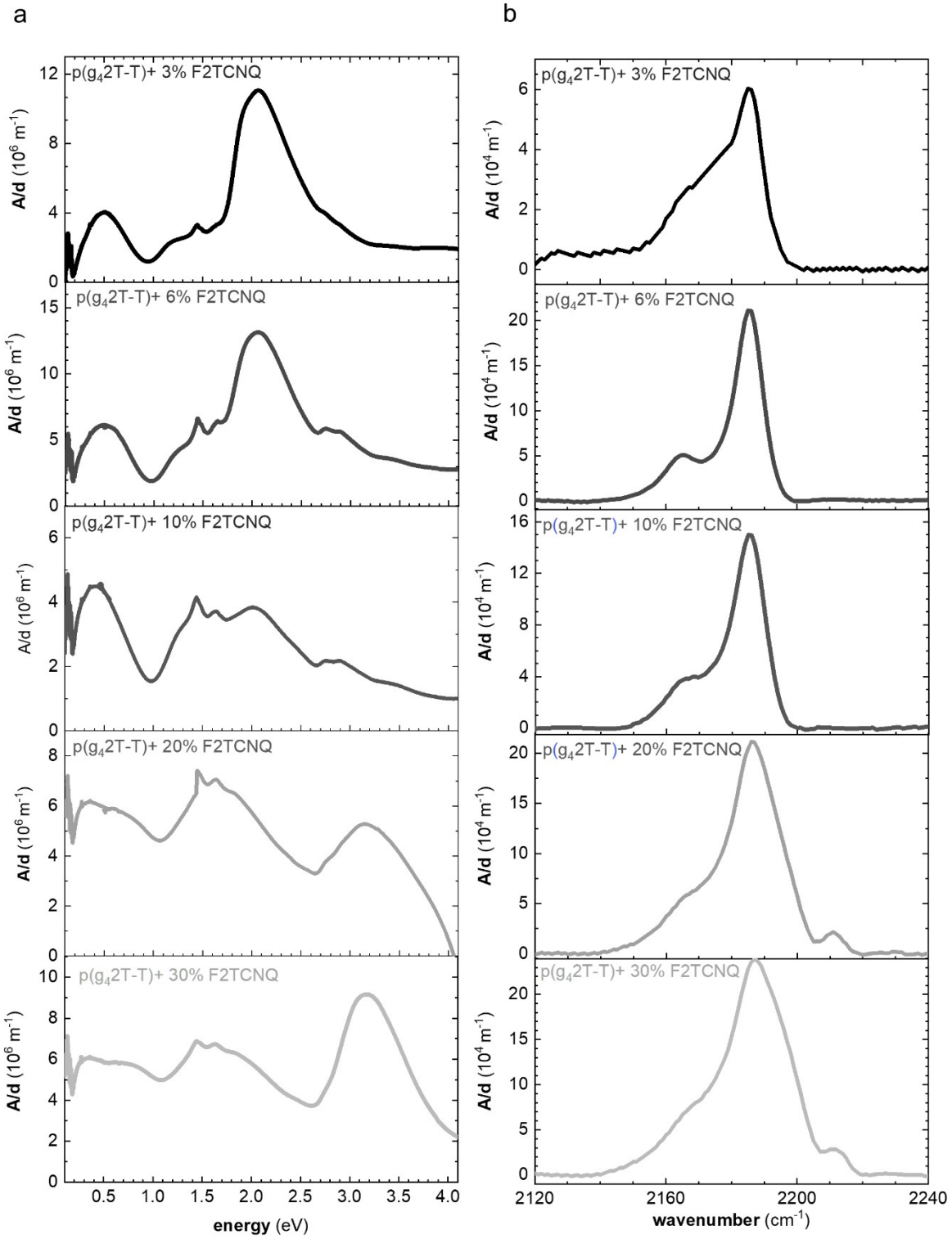

Fig. S8. a) UV-vis and (b) Transmission FTIR absorbance spectra, with the absorbance A normalized by the film thickness d, of p($g_4$2T-T) doped with 3 mol%, 6 mol%, 10 mol%, 20 mol% and 30 mol% F2TCNQ (grey).

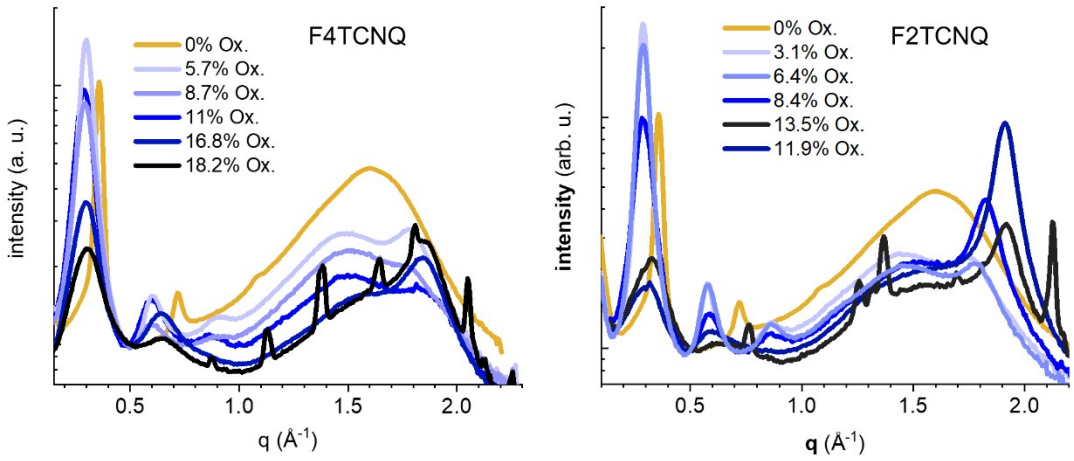

Fig. S9 X-ray diffractograms of neat p($g_4$2T-T) (yellow) and p($g_4$2T-T) doped with F4TCNQ and F2TCNQ (blue) recorded for bulk samples using transmission WAXS.

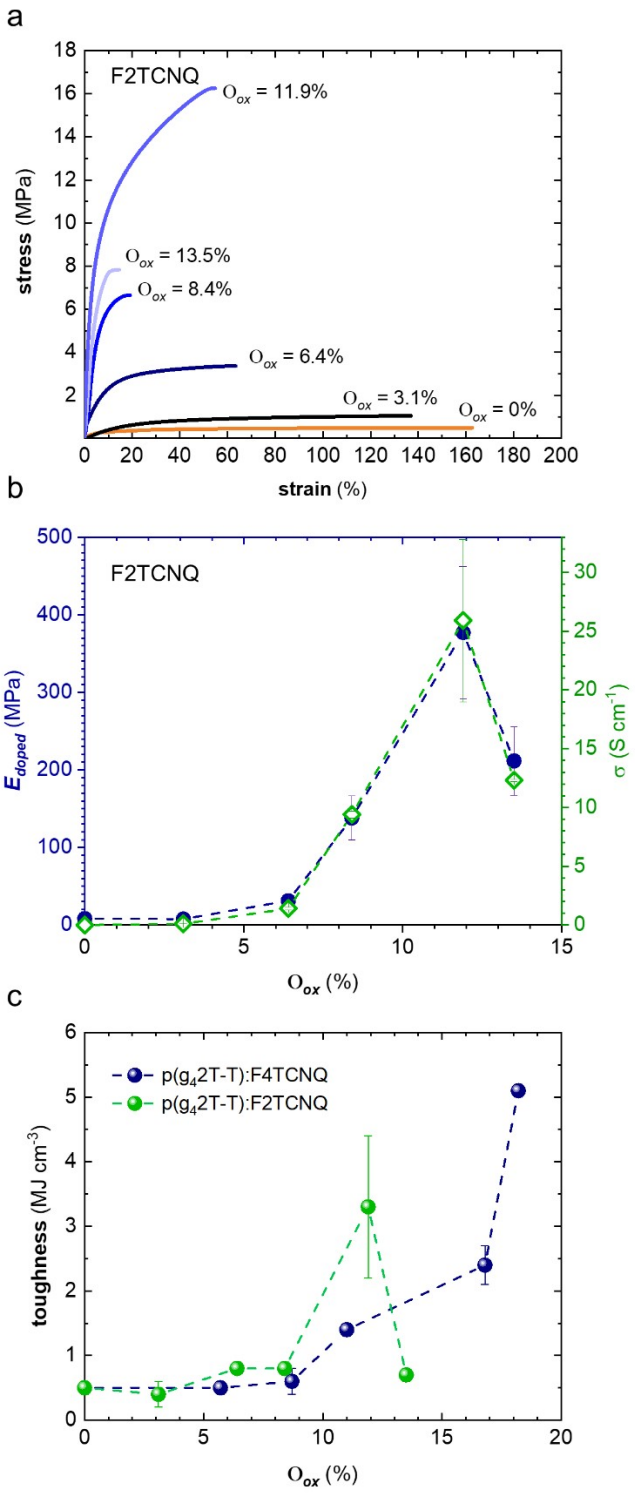

Fig. S10. (a) Stress-strain curves recorded at room temperature by tensile deformation of free-standing samples of neat p(g$_4$2T-T) (orange) and the polymer doped with F2TCNQ (blue) resulting in an oxidation level per thiophene ring O_{ox} ranging from 3.1 to 13.5 %; (b)

Young's modulus E (blue) and conductivity σ (green) of p($g_4$2T-T) doped with F2TCNQ; (c) toughness of p($g_4$2T-T) doped with F4TCNQ (blue) and F2TCNQ (green).

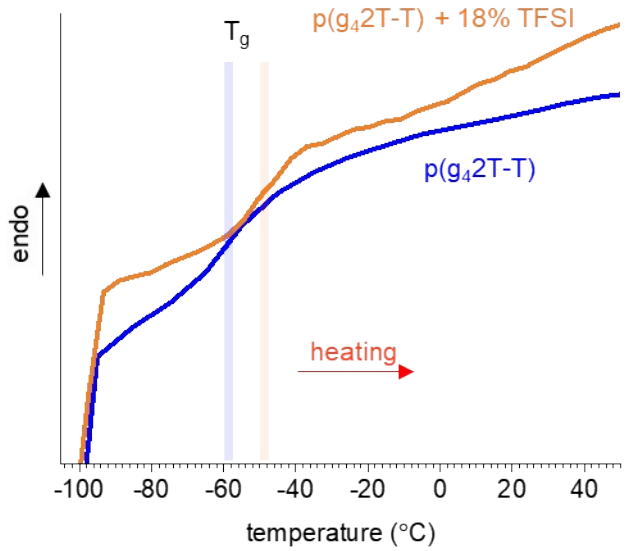

Figure S11. Glass transition temperatures of neat p($g_4$2T-T) (blue) and p($g_4$2T-T) co-processed with 18 mol% TFSI (orange) are highlighted in DSC heating thermograms.

Table S1. Charge per oligomer and counterion used for the molecular dynamics (MD) simulations, each involving 200 oligomers with four g_4(2T-T) repeat units; oxidation level $O_{ox} = N/12$.

charge *N* per oligomer	O_{ox} (%)	**charge of F4TCNQ counterion**	**number of F4TCNQ molecules**
0	0	-	0
+1	8.3	-1	200
+1	8.3	-2	100
+2	16.7	-1	400
+4	33.3	-1	800

Table S2. Electrical and mechanical properties of p($g_4$2T-T) doped with F4TCNQ or F2TCNQ: Oxidation level O_{ox}, Young's modulus E, strain at break ε_b, toughness K, electrical conductivity σ, total number of charges N_p, total number of dopant molecules N_{dopant} and ionization efficiency $\eta_{ion} = N_p/N_{dopant}$. For 3 and 6 mol% dopant O_{ox} was estimated by assuming that each dopant molecule undergoes charge transfer; in case of F4TCNQ the relative intensity of the absorption peaks was compared with FTIR signals recorded for solutions of the lithium and dilithium salt of F4TCNQ. For 10-30 mol% dopant O_{ox} was estimated by comparing the intensity of the FTIR absorption around 2190 cm^{-1} with the intensity recorded for 6 mol% dopant, for which the number of anions was known.

mol% dopant	O_{ox} (%)	E (MPa)	ε_b (%)	K (MJ m^{-3})	σ (S cm^{-1})	N_p (10^{26} m^{-3})	N_{dopant} (10^{26} m^{-3})	η_{ion} (%)
p($g_4$2T-T)								
0	0	8 ± 2	130 ± 43	0.5 ± 0.1	-	-	-	-
p($g_4$2T-T) + F4TCNQ								
3	5.7 ± 0.1	24 ± 4	30 ± 5	0.5 ± 0.1	0.3 ± 0.1	1.6	0.85	183
6	8.7 ± 0.1	53 ± 6	29 ± 8	0.6 ± 0.2	5.0 ± 0.3	2.4	1.75	137
10	11.0 ± 0.2	148 ± 20	30 ± 2	1.4 ± 0.1	30.4 ± 2.1	3.1	3.05	100
20	16.8 ± 0.3	207 ± 6	24 ± 3	2.4 ± 0.3	42.2 ± 1.1	4.6	6.86	67
30	18.2 ± 0.3	232 ± 16	54 ± 3	5.1 ± 0.1	51.8 ± 2.9	5.0	10.3	43
p($g_4$2T-T) + F2TCNQ								
3	3.1 ± 0.1	8 ± 2	93 ± 20	0.4 ± 0.2	0.1 ± 0.1	0.85	0.85	100
6	6.4 ± 0.1	31 ± 2	50 ± 10	0.8 ± 0.1	1.4 ± 0.1	1.75	1.75	100
10	8.4 ± 0.1	138 ± 28	17 ± 3	0.8 ± 0.1	9.4 ± 0.3	2.3	3.05	76
20	11.9 ± 0.2	377 ± 85	35 ± 10	3.3 ± 1.1	25.9 ± 6.9	3.3	6.86	48

30	13.5 ± 0.2	212 ± 44	12 ± 1	0.7 ± 0.1	12.3 ± 0.1	3.7	10.3	32